Semiconductor-Metal Nanoparticle Molecules: Hybrid Excitons and the Nonlinear Fano Effect

Wei Zhang,[1] Alexander O. Govorov,[1] and Garnett W. Bryant[2]
[1]Department of Physics and Astronomy, Ohio University, Athens, Ohio 45701-2979, USA
[2]National Institute of Standards and Technology, Gaithersburg, Maryland 20899-8423, USA
(Received 17 June 2006; published 4 October 2006)

Modern nanotechnology opens the possibility of combining nanocrystals of various materials with very different characteristics in one superstructure. Here we study theoretically the optical properties of hybrid molecules composed of semiconductor and metal nanoparticles. Excitons and plasmons in such a hybrid molecule become strongly coupled and demonstrate novel properties. At low incident light intensity, the exciton peak in the absorption spectrum is broadened and shifted due to incoherent and coherent interactions between metal and semiconductor nanoparticles. At high light intensity, the absorption spectrum demonstrates a surprising, strongly asymmetric shape. This shape originates from the coherent internanoparticle Coulomb interaction and can be viewed as a nonlinear Fano effect which is quite different from the usual linear Fano resonance.

DOI: 10.1103/PhysRevLett.97.146804 PACS numbers: 73.21.La, 71.35.Cc, 73.90.+f

Modern nanoscience involves both solid-state nanostructures and biomaterials. Using biomolecules as linkers, solid-state nanocrystals with modified surfaces can be assembled into superstructures with unique physical properties. Building blocks of these superstructures are nanowires, semiconductor quantum dots (SQDs), metal nanoparticles (MNPs), proteins, etc. [1,2]. To date, several interesting phenomena in bioconjugated colloidal nanocrystals, such as energy transfer [2], local field enhancement [3], and thermal effects [4,5], have been explored. In parallel with bioassembly, self-organized growth of epitaxial SQDs has become well developed. Self-assembled SQDs have excellent optical quality and atomically sharp optical lines [6]. This capability for nanocrystal, biomaterial, or epitaxial assembly [7,8] opens up the fabrication of complex hybrid superstructures that could exploit the discrete optical response of excitons in semiconductor nanosystems and the strong optical response of plasmons in MNPs.

In this Letter, we reveal novel unusual optical properties that arise in hybrid MNP-SQD molecules and motivate experiments to investigate these properties. Hybrid molecules have already been bioassembled and studied at room temperature (T) by several groups [2–4]. Hybrid MNP-SQD complexes can also potentially be realized with epitaxial SQDs [8]. The experimental methods to study such nanostructures include photoluminescence and absorption spectroscopies [6] and Raleigh scattering. While the effect of energy transfer from SQDs to MNPs can be observed at room T, the fine-scale coherent effects of internanocrystal interaction can become accessible only at low T.

In this Letter, we study the optical properties of hybrid structure composed of a MNP and a SQD. We explore both the linear regime (for weak external field) and the nonlinear regime (for strong external field). The basic excitations in the MNP are the surface plasmons with a continuous spectrum. In SQDs, the excitations are the discrete interband excitons. In the hybrid structure, there is no direct tunneling between the MNP and the SQD. However, long-range Coulomb interaction couples the excitons and plasmons and leads to the formation of hybrid excitons and to Förster energy transfer. The effect of coupling between excitons and plasmons becomes especially strong near resonance when the exciton energy lies in the vicinity of the plasmon peak. The coupling between the continuum excitations and the discrete excitations also leads to a novel effect that we call a nonlinear Fano effect. We should note that the usual Fano effect was introduced for the linear regime [9]. Here we describe a nonlinear Fano effect which appears at a high intensity of light when the SQD becomes strongly excited. This nonlinear Fano effect comes from interference between the external field and the induced internal field in the hybrid molecule. It appears at high intensities when the degree of coherence in the system becomes strongly increased, because the Rabi frequency starts to exceed the exciton broadening. A different type of nonlinear Fano resonance was found in Ref. [10].

We now consider a hybrid molecule composed of a spherical MNP of radius a and a spherical SQD with radius r in the presence of polarized external field $E = E_0 \cos(\omega t)$, where the direction of polarization is specified below. The center-to-center distance between the two nanoparticles is R (see the inset in Fig. 1). For the description of the MNP, we use classical electrodynamics and the quasistatic approach. For the SQD, we employ the density matrix formalism and the following model for a spherical SQD. Because of its symmetry, a spherical SQD has three bright excitons with optical dipoles parallel to the direction α, where α can be x, y, and z [11]. Using the symmetry of the molecule and a linearly polarized internal field, we can obtain the appropriate Hamiltonian [12]

$$\hat{H}_{\mathrm{SQD}} = \sum_{i=1,2} \epsilon_i c_i^+ c_i - \mu E_{\mathrm{SQD}} (c_1^+ c_2 + c_2^+ c_1), \quad (1)$$

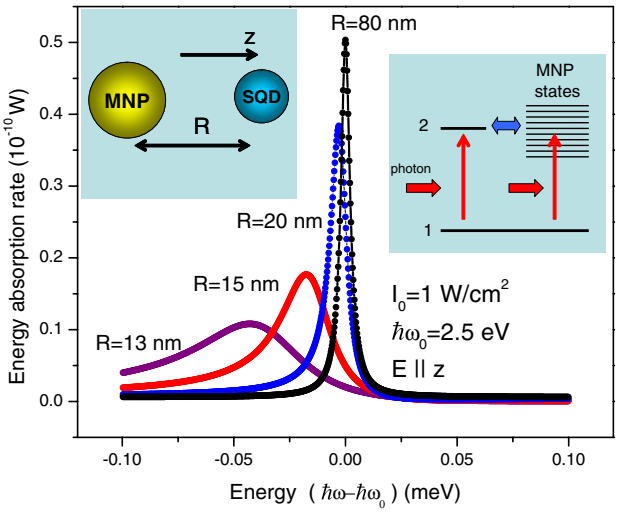

FIG. 1 (color online). Energy absorption spectra in the weak field regime for different interparticle distances. The light intensity is 1 W/cm^2. ω is the light frequency. $\hbar\omega_0$ is the bare exciton energy. $\hbar\Omega_0 = 3.3 \times 10^{-4}$ meV. The left inset shows a model. Right inset: Quantum transitions in the system; the vertical (horizontal) arrows represent light (Coulomb)-induced transitions.

where c_1^+ and c_2^+ are the creation operators for the vacuum ground state and the α-exciton state, respectively, μ is the interband dipole matrix element, $E_{\rm SQD}$ is the total field felt by the SQD, $E_{\rm SQD} = E + (s_\alpha P_{\rm MNP}/\varepsilon_{\rm eff1} R^3)$, with $\varepsilon_{\rm eff1} = (2\varepsilon_0 + \varepsilon_s)/3\varepsilon_0$, ε_0 and ε_s are the dielectric constants of the background medium and SQD, respectively, E is the external field, and $s_\alpha = 2(-1)$ for electric field polarizations $\alpha = z(y, x)$. The z direction corresponds to the axis of the hybrid molecule. The dipole $P_{\rm MNP}$ comes from the charge induced on the surface of the MNP. It depends on the total electric field which is the superposition of external field and the dipole field due to the SQD, $P_{\rm MNP} = \gamma a^3[E + (s_\alpha P_{\rm SQD}/\varepsilon_{\rm eff2} R^3)]$, where $\gamma = (\varepsilon_m(\omega) - \varepsilon_0)/[2\varepsilon_0 + \varepsilon_m(\omega)]$, $\varepsilon_{\rm eff2} = (2\varepsilon_0 + \varepsilon_s)/3$, and $\varepsilon_m(\omega)$ is the dielectric constant of the metal. The dipole of the SQD is expressed via the off-diagonal elements of the density matrix: $P_{\rm SQD} = \mu(\rho_{21} + \rho_{12})$ [12]. These matrix elements should be found from the master equation:

$$\frac{d\rho_{ij}}{dt} = \frac{i}{\hbar}[\rho, H_{\rm SQD}]_{ij} - \Gamma_{ij}\rho_{ij}, \qquad (2)$$

where the diagonal and off-diagonal relaxation matrix elements are $\Gamma_{12} = \Gamma_{21} = 1/T_{20}$ and $\Gamma_{22} = -\Gamma_{11} = 1/\tau_0$, respectively [12]. Here τ_0 includes the nonradiative decay via the dark states. We note that the above procedure treats the internanoparticle interaction in the self-consistent way. To solve the coupled system, we separate the high frequency part and write ρ_{12} and ρ_{21} as $\rho_{12} = \bar\rho_{12} e^{i\omega t}$ and $\rho_{21} = \bar\rho_{21} e^{-i\omega t}$. Applying the rotating wave approximation, we obtain the equations for steady state. Letting $\bar\rho_{21} = A + Bi$ and $\Delta = \rho_{11} - \rho_{22}$, we come to the system of nonlinear equations

$$A = -\frac{(\Omega_I + K\Omega_R)T_2}{1 + K^2}\Delta, \qquad B = \frac{(\Omega_R - K\Omega_I)T_2}{1 + K^2}\Delta,$$
$$(1 - \Delta)/\tau_0 = 4\Omega_R B - 4\Omega_I A - 4G_I(A^2 + B^2), \qquad (3)$$

where $K = [(\omega - \omega_0) + G_R\Delta]T_2$, $\omega_0 = (\varepsilon_2 - \varepsilon_1)/\hbar$, $1/T_2 = 1/T_{20} + G_I$, $G = s_\alpha^2 \gamma a^3 \mu^2/\hbar\varepsilon_{\rm eff1}\varepsilon_{\rm eff2} R^6$, $G_R = {\rm Re}[G]$, $G_I = {\rm Im}[G]$, $\Omega_{\rm eff} = \Omega_0[1 + s_\alpha\gamma(\frac{a}{R})^3]$, $\Omega_0 = \mu E_0/2\hbar\varepsilon_{\rm eff1}$, and $\Omega_R = {\rm Re}[\Omega_{\rm eff}]$, $\Omega_I = {\rm Im}[\Omega_{\rm eff}]$. Here $\Omega_{\rm eff}$ is the Rabi frequency of the SQD renormalized due to the dipole interaction with the plasmon of the MNP.

For a weak external field, we obtain the following steady state solution in the analytical form $\bar\rho_{12} = -\{\Omega_{\rm eff}/[(\omega - \omega_0 + G_R) - i(\Gamma_{12} + G_I)]\}$. The plasmon-exciton interaction leads to the formation of a hybrid exciton with shifted exciton frequency and decreased lifetime determined by G_R and G_I, respectively. In other words, the long-range Coulomb interaction leads to incoherent energy transfer via the Förster mechanism with energy transfer rate G_I. The exciton shift G_R shows that the interaction is partially coherent. A similar theoretical formalism for Förster transfer was successfully used to describe available experiential data [4,11]. For a strong field, the effective local fields on MNP and SQD ($E_{\rm SQD}$) are nonlinear, which has important consequences.

Energy absorption.—The energy absorption rate is $Q = Q_{\rm MNP} + Q_{\rm SQD}$, where the rate of absorption in the MNP and SQD are $Q_{\rm MNP} = \langle \int \mathbf{j}\mathbf{E} dV \rangle$, where $\mathbf{j}$ is the current, $\langle \cdots \rangle$ is the average over time, and $Q_{\rm SQD} = \hbar\omega_0\rho_{22}/\tau_0$. As an example, we consider a Au MNP with radius $a = 7.5$ nm. We use the bulk dielectric constant of Au $\varepsilon_m(\omega)$ taken from Ref. [13], $\varepsilon_0 = 1$, and $\varepsilon_s = 6.0$. The bare exciton frequency ω_0 is chosen to be 2.5 eV, close to the surface plasmon resonance of the Au MNP. Typically, the plasmon peak is very broad compared with the bare exciton peak; thus, a small detuning of the frequencies should have no important effect. Both the plasmon resonant frequency and the bare exciton frequency can be tuned in a wide range of energies (from blue to red) by changing the size and composition of the SQD/MNP. For the relaxation times and dipole moment, we take $\tau_0 = 0.8$ ns, $T_{20} = 0.3$ ns, and $\mu = er_0$, with $r_0 = 0.65$ nm.

In Fig. 1, we show the total energy absorption rate versus frequency. For weak incident light ($I_0 = 1$ W/cm^2), the energy absorption peak shifts and broadens for small interparticle separations R. This behavior of the optical spectrum for relatively small R reflects the formation of the hybrid exciton with a shifted frequency and shortened lifetime. In current experiments on epitaxial SQDs, the width of the exciton peak can be as small as a few μeV [6]. In our results in Fig. 1, the frequency shift is about 40 μeV for small separations $R \approx 15$ nm.

Figure 2 shows the energy absorption in the strong field regime. We find an asymmetrical Fano shape and substantial suppression of energy absorption. This striking asymmetry originates from the Coulomb coupling and vanishes at large R (see Fig. 2).

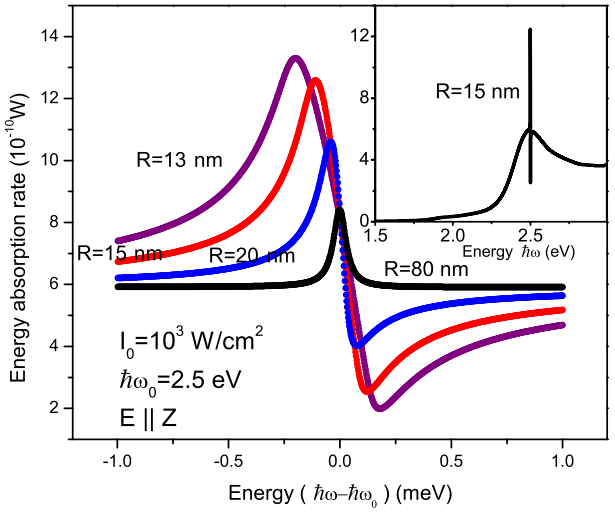

FIG. 2 (color online). Energy absorption spectra in the strong field regime for different interparticle distances. $\hbar\Omega_0 = 0.0106$ meV. The inset is the energy absorption for $R = 15$ nm for a wider frequency regime; the exciton feature is within the plasmon peak.

In the usual linear Fano effect, the absorption intensity becomes zero for a particular frequency due to the interference effect [9]. Here we find a nonvanishing energy absorption at any light frequency. This is due to the nonlinear nature of the interference effect in the hybrid molecule. A more qualitative discussion will be provided later. Again we see a redshift of the resonant frequency. The shift is now 1 order of magnitude larger than the energy resolution limit.

In Fig. 3, we show the polarization dependence. The Fano absorption intensity has the opposite shape for the electric field polarizations along the z and $x(y)$ directions. The shape reversal due to polarization happens in a frequency window of 1 meV and should be an observable experimental signature.

We see that the effective field applied to MNP and SQD is the superposition of the external field and the induced internal field. The interference between the external field and the internal field leads to the asymmetric Fano shape. Enhancement or suppression of the effective field depends on the polarization [s changes sign for the polarizations z and $x(y)$]. So, the polarization dependence is also a result of interference of the external field and the induced internal field.

Rayleigh scattering.—We use the standard method to calculate Rayleigh scattering intensity, which is valid when the size of the scattering objects is much smaller than the wavelength of incident light: $dI/d\Omega = P_0 \sin^2(\theta)$, where the angle θ is measured from the direction of the induced dipole and $P_0 = (ck^4/\hbar)(P_{\mathrm{SQD}} + P_{\mathrm{MNP}})^2$.

Figure 4 shows the Rayleigh scattering in the linear and nonlinear regimes. The interaction between the SQD and MNP leads to a shift of the peak of scattering intensity in Fig. 4 and to the polarization dependence (see inset in Fig. 4).

As discussed above, experiments could be performed on self-assembled SQDs coupled to MNPs. The inset in Fig. 5 shows a schematic of such a system with $\varepsilon_0 = \varepsilon_s = 12$ with the MNP embedded in the barrier material that defines the SQD (here we still assume a spherical SQD for simplicity). Again we see a clear asymmetry which is strong even in the linear regime. This behavior was found for parameters typical of a self-assembled SQD. The electric field polarization was chosen along the $y(x)$ directions (inset in Fig. 5). The strong advantage of self-assembled SQDs is that an exciton in such systems exhibits a very narrow line [6].

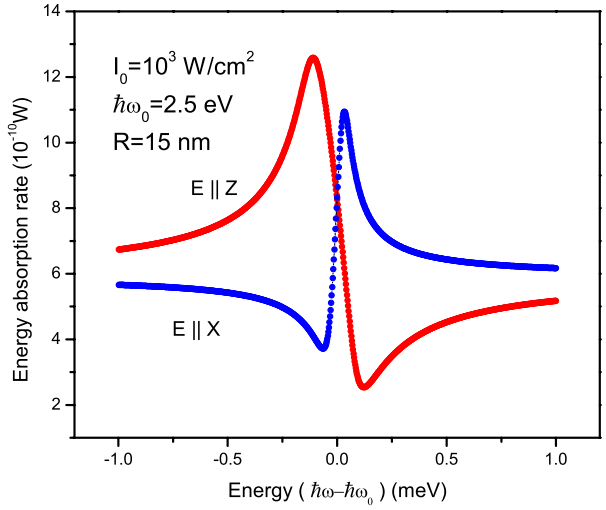

FIG. 3 (color online). Polarization dependence for the energy absorption.

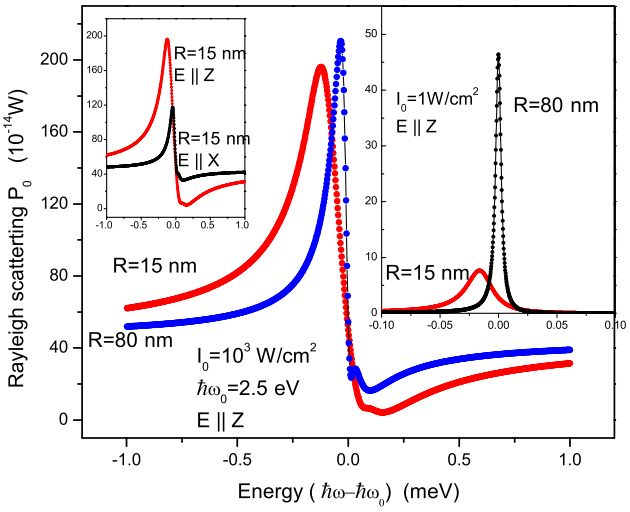

FIG. 4 (color online). Rayleigh scattering intensity P_0. The main panel is for the strong field regime. Right inset: Scattering intensity P_0 for the weak field regime. Left inset: Intensity P_0 for different polarizations in the strong field regime.

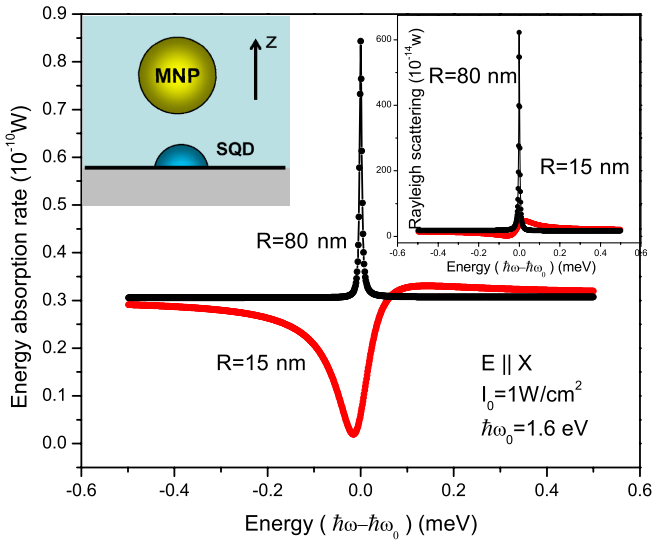

FIG. 5 (color online). Energy absorption and Rayleigh scattering (right inset) for a system with a self-assembled quantum dot in the weak field regime. $\hbar\Omega_0 = 4.8 \times 10^{-4}$ meV. Left inset: Schematics of a hybrid molecule. The self-assembled SQD is formed at the interface of two materials.

Nonlinear Fano effect.—In the linear regime, the absorption peak can have almost a Lorentzian shape (Fig. 1). Here we describe a nonlinear Fano effect. This effect manifests itself as a strong asymmetry of the absorption peak at high light intensities.

The energy absorption in the weak field regime or strong field regime is

$$Q = C\Omega_0^2\left(\frac{(K-q)^2}{1+K^2} + \alpha\frac{1}{1+K^2}\right) + \beta\frac{\hbar\omega_0}{1+K^2}. \quad (4)$$

Here $K = [(\omega - \omega_0) + G_R\Delta]T_2$, $q = s_\alpha\mu^2\Omega_R T_2\Delta/\hbar\varepsilon_{\text{eff}1}\varepsilon_{\text{eff}2}R^3\Omega_0$, and the coefficient $C = \frac{1}{6}(\frac{2\hbar}{\mu})^2 a^3\omega|3\varepsilon_0/(2\varepsilon_0 + \varepsilon_m)|^2\text{Im}[\varepsilon_m]$. For the weak field regime, $\alpha = [1/(1 + G_I T_{20})]^2$ and $\beta = |4\Omega_{\text{eff}}|^2(T_2^2/T_{20})$, and for the strong field regime, $\alpha = 1$ and $\beta = 1/2\tau_0$.

In the weak field regime ($\Omega_0 \ll 1/T_2, 1/\tau$), Q has the Fano function form in the limit $T_{20} \to \infty$. (This was also checked by numerical calculations not shown here.) For a finite T_{20}, the finite broadening of the exciton peak may destroy the linear Fano effect and we see a symmetric peak (Fig. 1). For self-assembled SQD, the Fano asymmetry is well expressed even in the linear regime (Fig. 5). It is interesting to note that, in the regime of the symmetric peak (see, e.g., Fig. 1), an exciton frequency shift $\sim G_R \sim 1/R^6$. However, in the regime of the nonlinear Fano effect (Fano shapes in Figs. 2 and 3), the resonant frequency shift $\sim 1/R^3$ and is field dependent. Another interesting feature of the nonlinear regime is that the absorption never vanishes, even in the limit $T_{20}, \tau_0 \to \infty$.

Qualitatively, the nonlinear Fano effect can be explained as follows. When the SQD is strongly driven ($\Omega_0 \gg 1/T_2$, $1/\tau$), the absorption peak becomes strongly suppressed, as in an atom [12]. For the MNP, we assume that the plasmon is not strongly excited. This is because of the very short lifetime of the plasmon (of the order of 10 fs). Simultaneously, the ac dipole moments of the MNP and SQD increase with increasing intensity. In this situation, the interference between two channels of plasmon excitation in the MNP [these channels correspond to the first and second terms in the total electric field in Eq. (3)] increases and the peak asymmetry is greatly enhanced. We should finally note that similar nonlinear effects can appear for a SQD coupled with a metal surface [14].

It is possible to show that the problem of Förster-like interaction between a SQD and a MNP is equivalent to the Fano problem [9]. To solve this problem, we can also use the density matrix formulation for a description of the plasmon excitations in a MNP and look at the interaction between continuum plasmon states and discrete exciton states directly, without employing a self-consistent approach.

In conclusion, we have studied the optical properties of a hybrid nanostructure composed of a MNP and a SQD. The interaction between the plasmon and the exciton leads to interesting effects such as Förster energy transfer, exciton energy shift, and interference. At a high light intensity, we find a novel nonlinear Fano resonance which has striking differences to the usual Fano effect.

We acknowledge helpful discussions with Dr. T. Klar. This work was supported by NIST and BNNT Initiative at Ohio University.

[1] Y. Cui *et al.*, Science **293**, 1289 (2001); Y. A. Yadong *et al.*, Nature (London) **437**, 664 (2005); E. Dulkeith *et al.*, Nano Lett. **5**, 585 (2005).
[2] J. Lee *et al.*, Nano Lett. **4**, 2323 (2004).
[3] K. T. Shimizu *et al.*, Phys. Rev. Lett. **89**, 117401 (2002).
[4] J. Lee *et al.*, Angew. Chem. **117**, 7605 (2005); K. T. Slock *et al.*, Supramol. Chem. **18**, 415 (2006); K. Ray, R. Badugu, and J. R. Lakowicz, J. Am. Chem. Soc. **128**, 8998 (2006).
[5] H. Richardson *et al.*, Nano Lett. **6**, 783 (2006).
[6] J. R. Guest *et al.*, Phys. Rev. B **65**, 241310(R) (2002); A. Högele *et al.*, Phys. Rev. Lett. **93**, 217401 (2004); H. Htoon *et al.*, Phys. Rev. Lett. **88**, 087401 (2002).
[7] Zh. M. Wang *et al.*, Appl. Phys. Lett. **86**, 143106 (2005); V. V. Chaldyshev, J. Appl. Phys. **97**, 024309 (2005).
[8] D. C. Driscoll *et al.*, Appl. Phys. Lett. **86**, 051908 (2005); U. Woggon *et al.*, Nano Lett. **5**, 483 (2005).
[9] U. Fano, Phys. Rev. **124**, 1866 (1961).
[10] A. E. Miroshnichenko *et al.*, Phys. Rev. E **71**, 036626 (2005).
[11] A. O. Govorov *et al.*, Nano Lett. **6**, 984 (2006).
[12] A. Yariv, *Quantum Electronics* (Wiley, New York, 1975).
[13] E. D. Palik, *Handbook of Optical Constant of Solids* (Academic, New York, 1985).
[14] See, e.g., K. J. Ahn and A. Knorr, Phys. Rev. B **68**, 161307 (2003).